Nickel(II) driven activity enhancement of donor-acceptor porous organic polymer for selective photoreduction of carbon dioxide

A John David, [a] Nandini M Gotgi, [b] Gopika Udayakumar, [a] A Hameed Ibrahim, [a] Abhilash Pullanchiyodan, [a]* Debashis Ghosh [c]* and Anjan Das [a]*

[a] Department of Chemistry, SRM Institute of Science and Technology, Kattankulathur, Chennai, Tamil Nadu, India, 603203
[b] Department of Chemistry, St. Joseph's University, 36 Lalbagh Road, Bengaluru-560027, Karnataka, India
[c] Department of Chemistry, R.D. & D.J. College, Munger 811201, Bihar, India

General

All the reagents were obtained from commercial suppliers and were used without further purification. Solvents were dried by slandered procedures. Thin layer chromatography was performed on Merck silica gel 60F254 plates and visualised by UV irradiation at 254 nm. Heating was performed using oil bath on a hotplate stirrer. ^{1}H NMR spectra were recorded on a Bruker AC400 (400 MHz) instrument. Chemical shifts are reported in ppm with respect to the residual solvent peaks, with multiplicities given as s = singlet, d = doublet, t = triplet, q = quartet, m = multiplet, br = broad. Coupling constants (J values) are quoted to the nearest 0.5 Hz with values in Hertz (Hz). Photochemical reaction was done using a high-power 470 nm LED light source (Model no: L-470-HP), MARUTEK (light power = 70 W/m^2). Light intensity was determined using a power meter. Gas samples were detected using a Gas Chromatographic instrument (Model no: 1100), Mayura Analytical LLP. Retention time of the gas samples was compared with canister samples (certified by Mayura Analytical LLP, accuracy ±0.2%). HCOOH was analyzed using HPLC (Model no: LC-2500C), SHIMADZU (column: X-bridge C18 3.5 m (150 x 4.6) mm) using mobile phases A (10 mM ammonium bicarbonate) and B (CH_3CN), flow rate: 1 mL/min. The quantification of H_2, CO, and HCOOH was done using calibration curves. Based on these curves, the detection limits for CO and CH_4 were determined to be 5 mL (i.e., 0.00015153 μmol) and 5 mL (0.0001503 μmol), respectively.

Thermogravimetric analysis (TGA): A thermogravimetric analyser was used to perform thermogravimetric analysis (TGA) at a ramp rate of 10°C min^{-1} between 30 °C and 900 °C in a N_2 environment. The samples were activated at 100 °C for 30 minutes prior to TGA to remove any remaining water.

Scanning Electron Microscopy (SEM) SEM analysis was performed using a high-resolution scanning electron microscope (Thermoscientific, Apreo S) operating at 18 kV. To prevent charge during SEM investigations, the samples were sputtered in aluminium foil sheet prior to imaging. A drop of dispersed samples (Ni@Py-DPEN and Py-DPEN) in ethanol was placed on an aluminium foil to create the samples. SEM combined with energy dispersive X-ray spectroscopy (EDS) was also used to record the elemental mapping of the Ni@Py-DPEN and Py-DPEN. In these instances, solid sample coating on a conductive, non-porous adhesive carbon strip was used to create the samples.

Transmission Electron Microscopy (TEM): The images were obtained using (JEOL Japan's JEM-2100 Plus) facility was used to acquire Transmission Electron Microscopy (TEM) pictures at a 200kV accelerating voltage. The samples were made by directly drop-casting them onto copper grids using a TEM window (TED PELLA, INC. 200 mesh) with ethanol scattered throughout.

X-ray Photoelectron Spectroscopy (XPS) analysis was carried out using PHI Versaprobe III was used to perform the X-ray Photoelectron Spectroscopy (XPS) investigation. When the angle between the analyzer and the sample surface was 90 °, the pass energies for the survey scan and the high-resolution scan were kept at 100 eV and 50 eV, respectively. First, the Fityk 1.3.1 software was used to evaluate and fit the deconvoluted spectra.

Inductively Coupled Plasma - Optical Emission Spectrometer (ICP-OES): Analysis was carried out by the Agilent Technologies instrument (Model no. 4210 MP-AES). The analytical wavelength for metal detection was selected based on intensity counts and background interference. Operating condition for ICP-OES are given as follow- [Coolant Flow-12 L/min, Auxiliary Flow-0.50 L/min, Nebulizer Flow-0.50 L/min, Carrier gas- Argon].

Ultraviolet-Visible Spectroscopy (UV-Vis): The powder solid samples were subjected to Ultraviolet-Visible Spectroscopy (UV-Vis) utilizing a quartz plate holder and LUZCHEM-LZC-4V.

FT-IR spectrometer: A Shimadzu IRTracer-100 FT-IR spectrometer was used to acquire FT-IR spectra. ATR mode was used to examine (Ni@Py-DPEN and Py-DPEN).

Synthesis of porous organic polymer (Ni@Py-DPEN):

Step:1 Synthesis of 1,3,6,8 tetra-(4-formylphenyl)pyrene (TFPPy): [1]

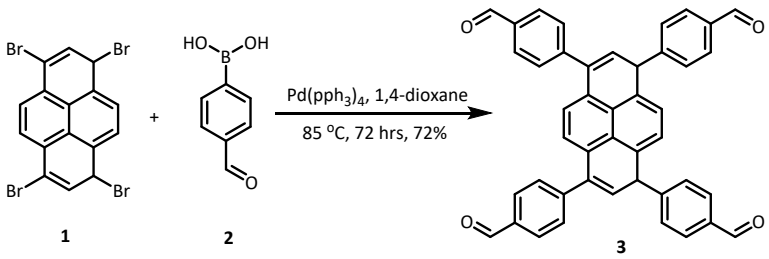

1 2 3

A two-neck round bottom flask charged with 1,3,6,8- Tetrabromopyrene **1** (754 mg, 1.45 mmol), 4-formylphenylboronic acid **2** (1.3 g, 8.7 mmol), tetrakis (triphenylphosphine) palladium (100 mg, 0.64 mmol) and potassium carbonate (2.1 g, 15 mmol) was added in dry 1, 4-dioxane (50 ml), then the mixture was heated in an inert atmosphere for 72 hrs at 85 ^{o}C. after that cooled down the reaction mass in to room temperature. Filtered the residue and washed with three time (3x30 ml) of acetone dry in the oven at 65 ^{o}C for 24 hrs to obtain TFPPY **3** as yellow solid (Yield 1.29 g, 72%); ^{1}H NMR (400 MHz, $CDCl_3$) δ 10.17 (s, 1H), 8.18 (s, 1H), 8.10 (d, *J* = 8.0 Hz, 2H), 8.04 (s, 1H), 7.87 (s, 1H), 7.86 (d, *J* = 8.1 Hz, 2H), 7.81 (d, *J* = 8.2 Hz, 1H).

Preparation of porous organic polymer (Py-DPEN): [2]

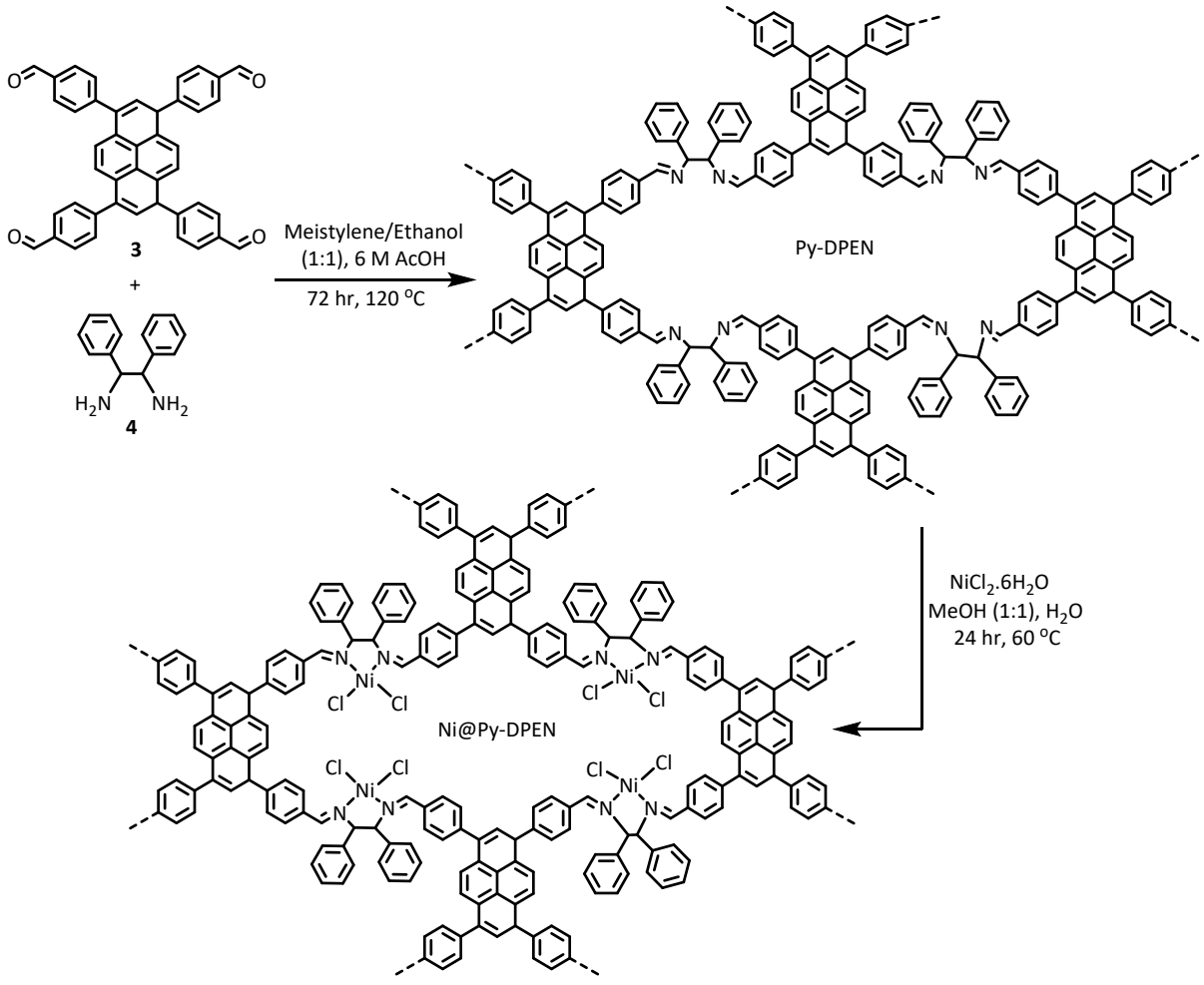

TFPPy **3** (100 mg, 0.162 mmol), 1, 2-diphenylethane-1, 2-diamine (DPEN) **4** (69 mg, 0.48 mmol), acetic acid (300 μL, 6 M), mesitylene (1 mL), and EtOH (1 mL) in a 1:1 ratio was added

to a 10 mL oven-dried sealed tube. The mixture was subjected to 2 minutes of ultrasonication, followed by flash-freezing at 77 K in a liquid nitrogen bath. Three freeze–pump–thaw cycles were carried out for degassing, after which the tube was sealed under nitrogen using a Schlenk line and vacuum pump. The sealed tube was then heated at 120 °C for 96 hours. After cooling to room temperature, the residue was washed three times with acetone, followed by three rounds of methanol washing. Finally, Soxhlet extraction with methanol was performed for two days. After oven-drying, Py-DPEN was obtained as an orange powder.

Ni@Py-DPEN was made heating the mixture of 30 mg of $NiCl_2.6H_2O$ and 50 mg of **Py-DPEN** in a 2 ml H_2O-EtOH (1:1) at 60 ^oC for 24 hrs. The resulting solid residue was then filtered, rinsed three times each with water and acetone, and vacuum-dried for an entire night at 120°C to obtain the **Ni@Py-DPEN** as dark brown powder. 1H NMR (400 MHz, CDCl3) δ 10.16 (s, 1H), 8.18 (s, 1H), 8.09 (d, J = 8.0 Hz, 2H), 8.04 (s, 1H), 7.99 (s, 1H), 7.86 (d, J = 8.1 Hz, 2H), 7.81 (d, J = 8.2 Hz, 1H).

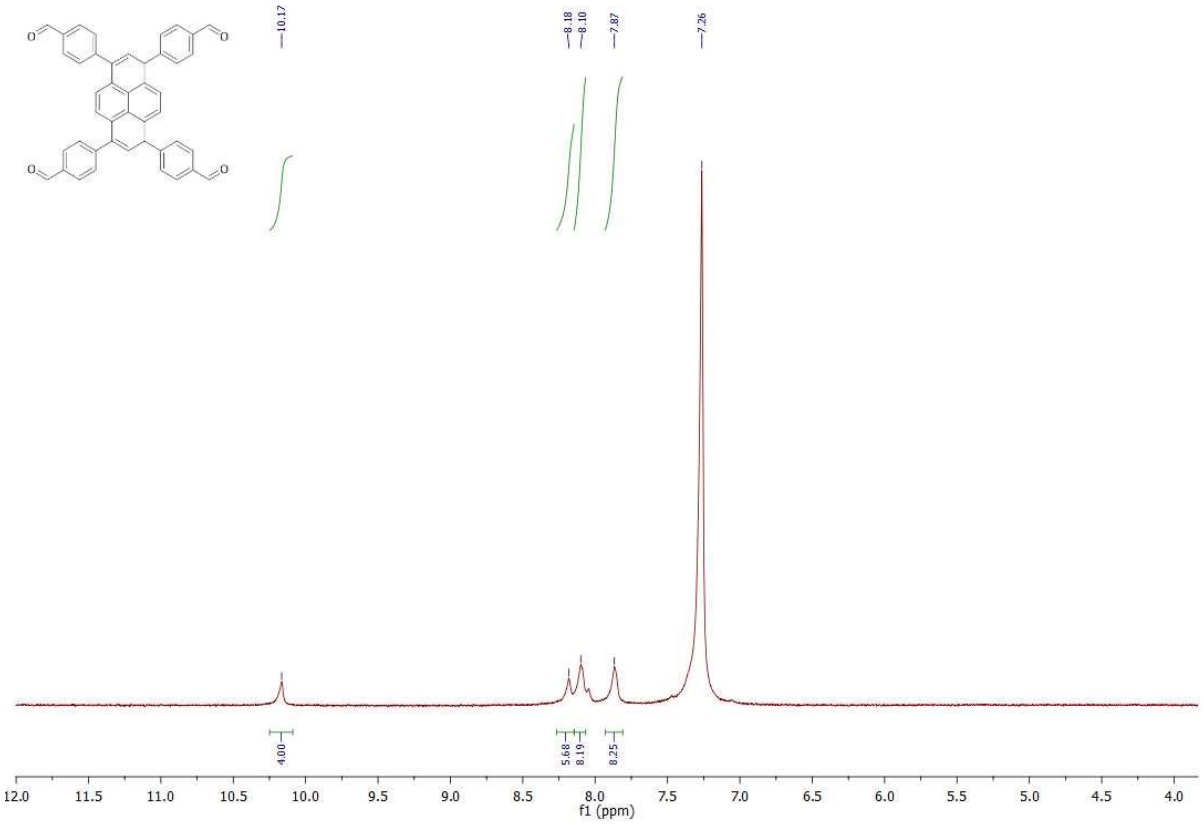

Figure S1. ^{1}H-NMR spectra of **TFPPy**

Characterizations of Materials:

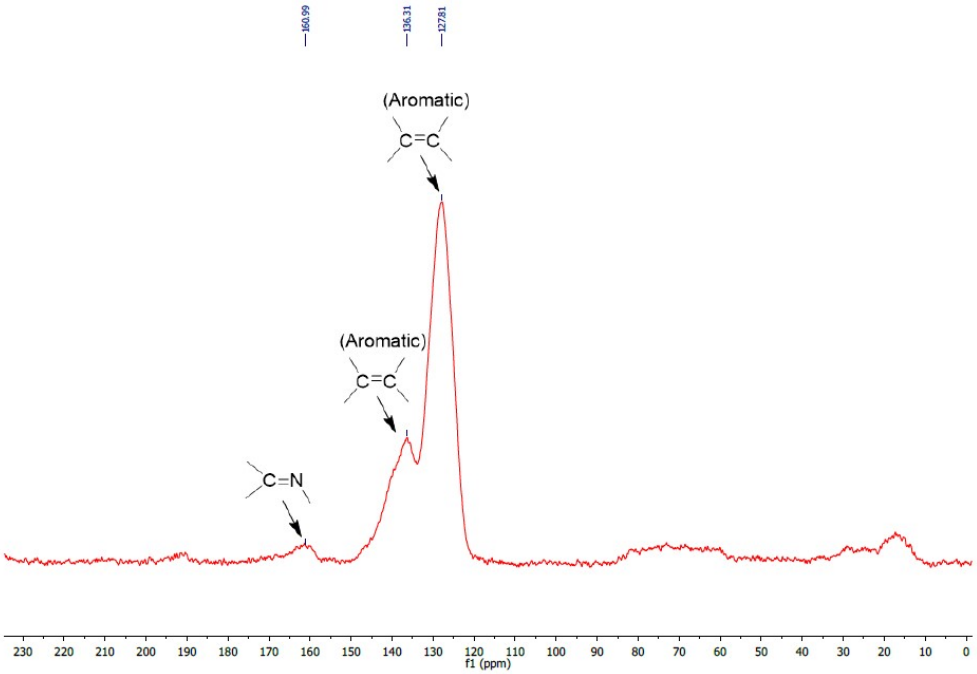

Figure S2. ^{13}CP-MAS spectra of Py-DPEN

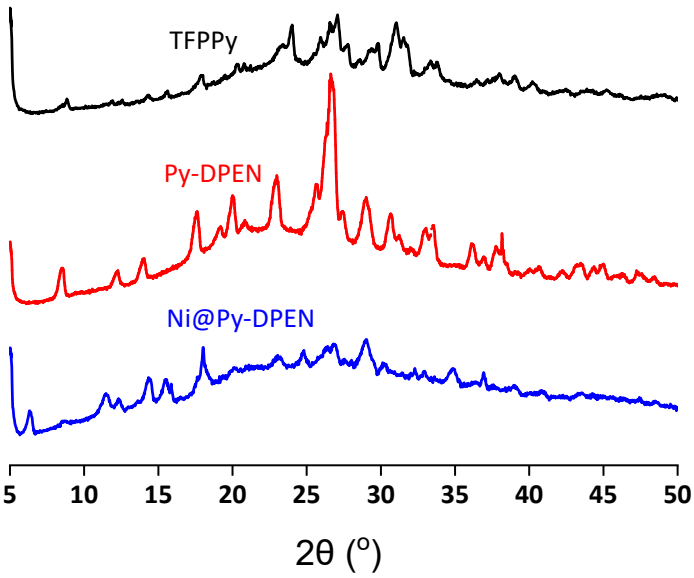

Figure S3. Powder XRD of TFPPy, Py-DPEN and Ni@Py-DPEN

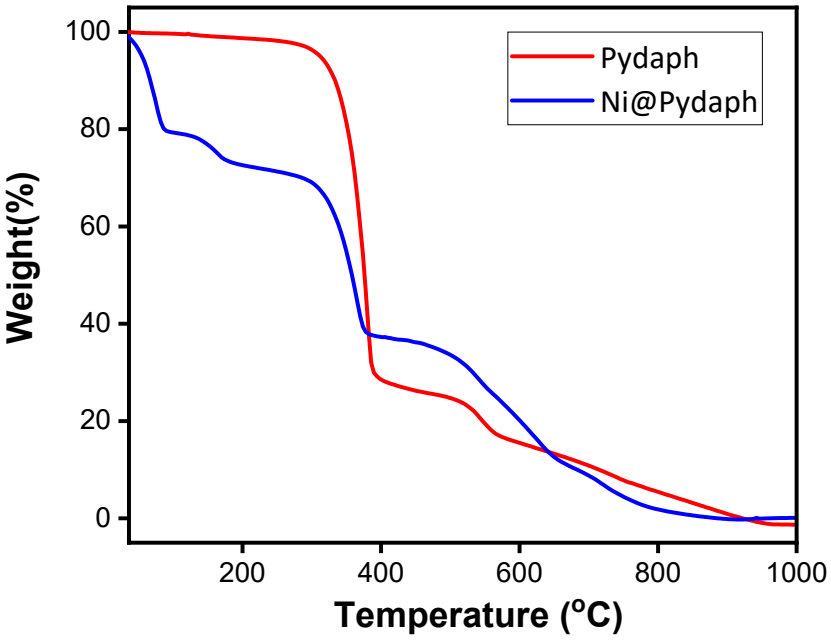

Figure S4. TGA analysis of Py-DPEN (red) and Ni@Py-DPEN (blue)

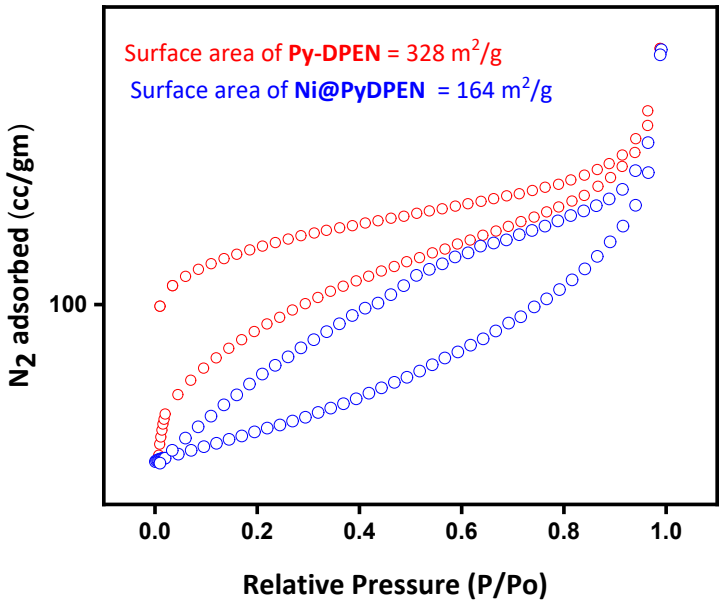

Figure S5. BET surface area analysis of Py-DPEN and Ni@Py-DPEN

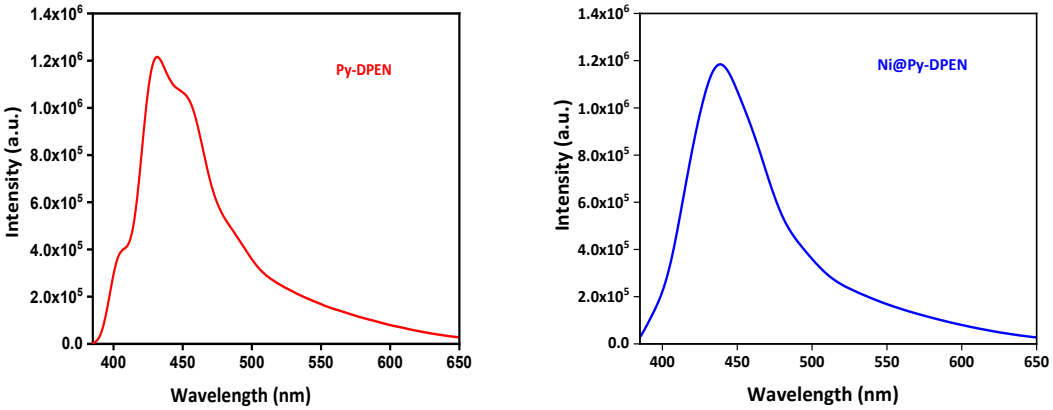

Figure S6. Emission Spectra of Py-DPEN and Ni@Py-DPEN

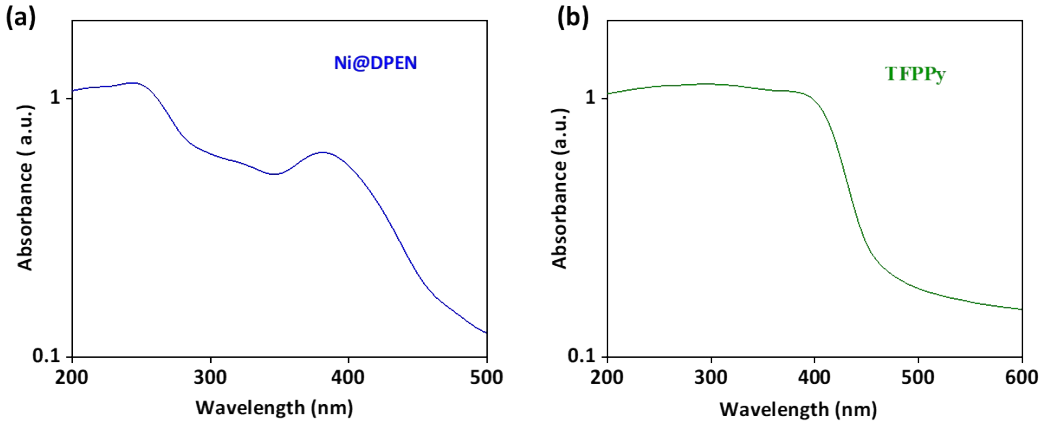

Figure S7. Solid UV- Spectra of Ni@DPEN and TFPPy

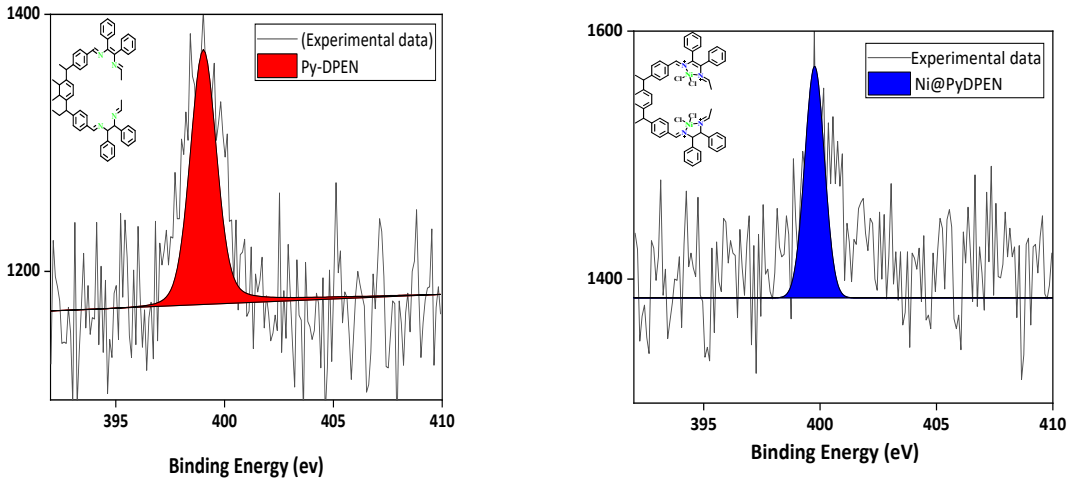

Figure S8. The XPS deconvoluted N1s spectra of Py-DPEN (red) and Ni@Py-DPEN (blue). The XPS analysis of the Py-DPEN and Ni metal loaded Py-DPEN POP revealed the deconvoluted N1s spectra where the red area represented N (from imine group) contribution, the red area represented N (Ni coordinated) contribution respectively.

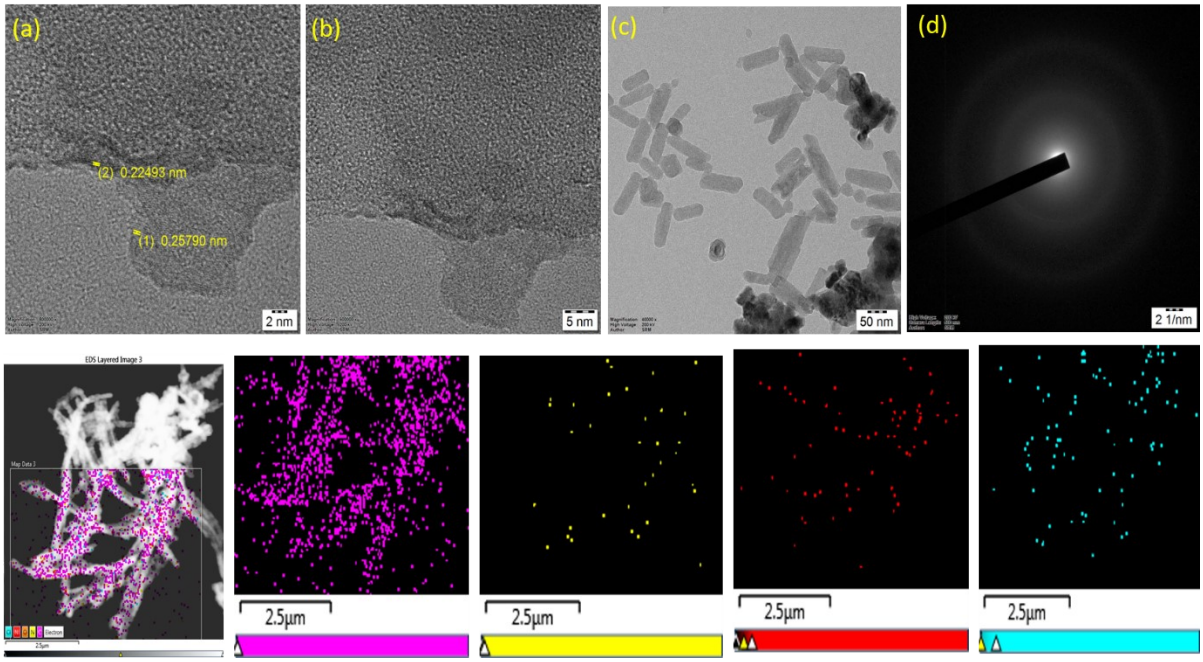

Figure S9. TEM images of Ni@Py-DPEN (a, b, c, d) and elemental analysis

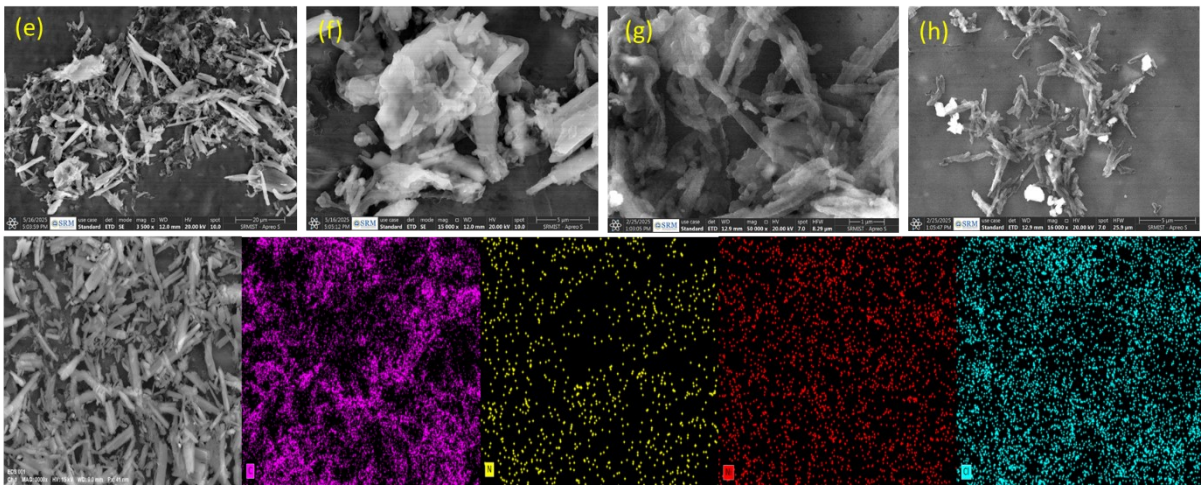

Figure S10. SEM images of Ni@Py-DPEN (e, f, g, h) and EDS analysis

Electrochemical measurement:

CV experiments were performed using a one compartment, three-electrode configuration, connected to a CHI6011E electrochemical workstation. Initially, 0.5 mg of the Ni@Py-DPEN (or Py-DPEN) was added in a 1 ml of HPLC grade CH_3CN, and then sonicated for 10 min and then drop casted onto glassy carbon electrode glassy carbon disk (0.071 cm^2) working electrode that was polished with alumina (0.05 µm) prior to use. The modified electrode was kept overnight prior use. a coil platinum wire as the counter electrode, and an $Ag/AgNO_3$ reference electrode, which was calibrated using $FeCp_2$ as the internal standard. Cyclic voltammograms were measured using 0.1 M $[n\text{-}Bu_4N][PF_6]$ as the supporting electrolyte in either Ar- or CO_2-saturated CH_3CN (CH_3CN-H_2O or CH_3CN-H_2O-TEOA in some cases) solutions at room temperature.

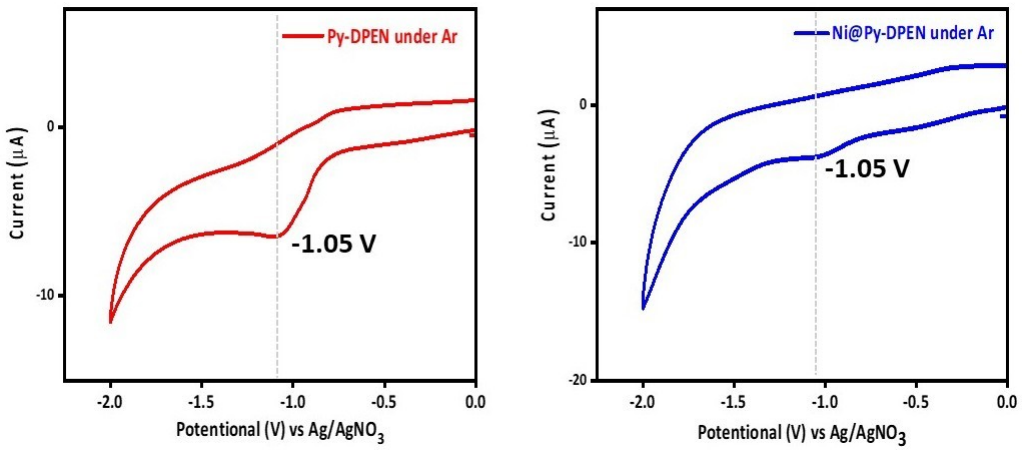

Figure S11. Cyclic voltammogram Py-DPEN POP (drop-casted on glassy carbon electrode) in CH_3CN-H_2O (9:1 v/v) under Ar atmospheres. For all measurements, 0.1 M $TBAPF_6$ was used as a supporting electrolyte, and $Ag/AgNO_3$ (10 mM, in CH_3CN) was taken as a reference electrode; Scan rate: 50 mV s^{-1}.

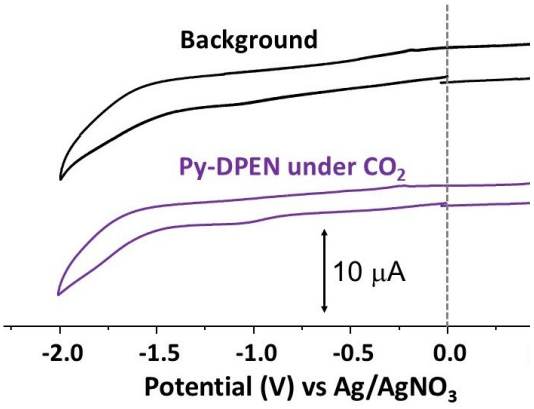

Figure S12. Cyclic voltammogram Py-DPEN POP (drop-casted on glassy carbon electrode) in CH_3CN-H_2O (9:1 v/v) under CO_2 atmospheres. For all measurements, 0.1 M $TBAPF_6$ was used as a supporting electrolyte, and $Ag/AgNO_3$ (10 mM, in CH_3CN) was taken as a reference electrode; Scan rate: 50 mV s^{-1}.

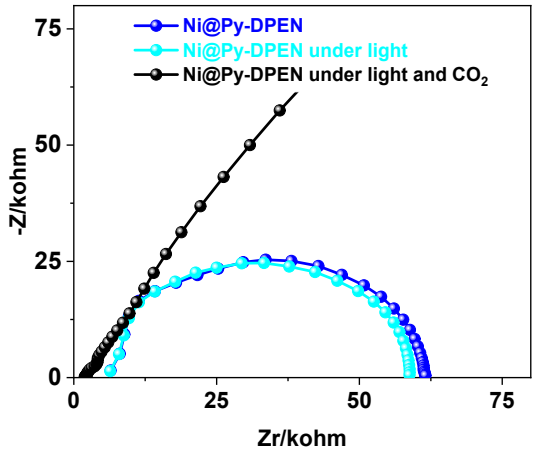

Figure S13. EIS Nyquist plot of Ni@Py-DPEN in the presence and absence of light (blue), under light, Ar atmosphere (sky blue), under light, CO_2 atmosphere (black).

Procedure for photochemical CO_2 reduction using Ni@PyDPEN in CH_3CN-TEOA (4:1) under CO_2 atmosphere:

First 10 mL of CH_3CN-TEOA (4:1, v/v) solution was prepared in a standard flask. From that 4 mL was transferred into the reaction quartz tube. Further, 3 mg of Ni@PyDPEN was added to the reaction. The reaction mixture was sonicated for 5 minutes and then bubbled with CO_2 for 10 minutes before sealing it with the airtight septum. The photo-irradiation was then

started using Blue LED (470 nm) light (power = 70 W/m^2) with constant stirring (800 rpm). The gas phase and solvent phases were tested at certain time interval. The gaseous products, CO and H_2, were analyzed by GC TCD (GC-1100, Mayura Analytical LLP). HCOOH was analysed by HPLC (SHIMADZU LC-2500C).

Procedure for photochemical CO_2 reduction using Ni@PyDPEN or PyDPEN in CH_3CN-H_2O-TEOA (9:1:2) under CO_2 atmosphere:

First prepare 10 mL of CH_3CN-H_2O (9:1 v/v) solution in a standard flask and then add 2 ml TEOA into it and shake well. From that 4 mL was transferred into the reaction quartz tube. Further, 3 mg of Ni@PyDPEN or PyDPEN was added to the reaction. The reaction mixture was sonicated for 5 minutes and then bubbled with CO_2 for 10 minutes before sealing it with the airtight septum. The photo-irradiation was then started using Blue LED (470 nm) light (power = 70 W/m^2) with constant stirring (800 rpm). The gas phase and solvent phases were tested at certain time interval. The gaseous products, CO and H_2, were analysed by GC TCD (GC-1100, Mayura Analytical LLP). HCOOH was analysed by HPLC (SHIMADZU LC-2500C).

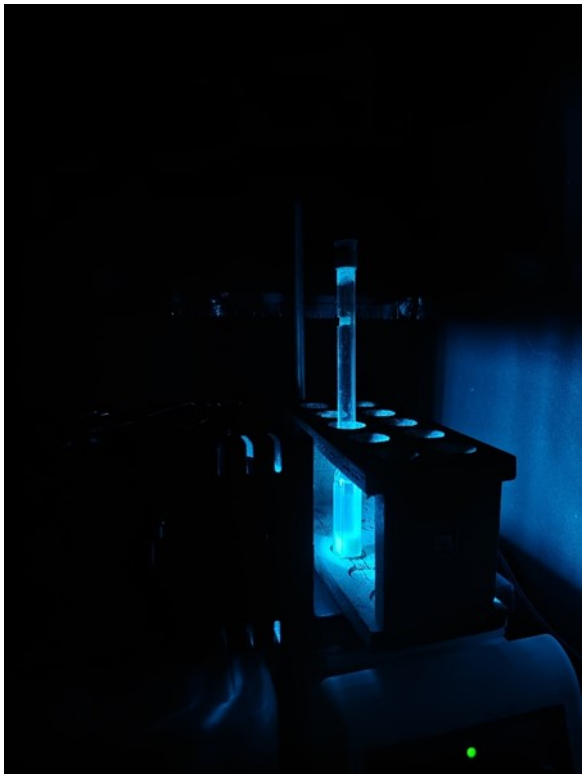

Figure S14. The reaction set up.

Photochemical reaction results

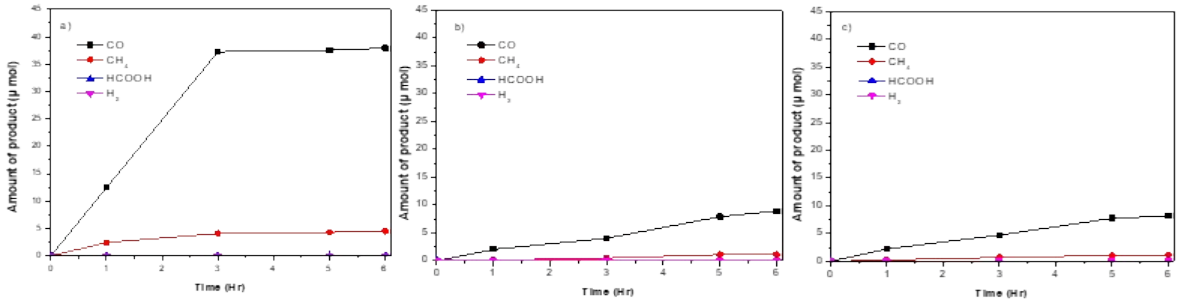

Figure S15. Time course profile of the reaction. Irradiated with blue LED at λ_{ex} = 470 nm (light power = 70 W/m^2). Formation of CO (■), CH_4 (●), HCOOH (▲), and H_2 (▲) during the photoirradiation to CO_2-saturated (a) CH_3CN-H_2O-TEOA (9:1:2 v/v, 4.0 mL) solutions containing Ni@Py-DPEN (3mg), (b) CH_3CN-H_2O-TEOA (9:1:2 v/v, 4.0 mL) solutions containing Py-DPEN (3mg), (c) CH_3CN-TEOA (4:1 v/v, 4.0 mL) solutions containing Ni@Py-DPEN POP (3 mg) in at 298 K.

Table S1. Photochemical results [a]

Entry	Catalyst [3mg]	Solvent system	Time (h)	Amount of CO/ μmol	Amount of CH_4 / μmol	S_{CO} (%)
1	Ni@Py-DPEN	CH_3CN-H_2O-TEOA (9:1:2)	6	38	4.5	89.4
2	Py-DPEN	CH_3CN-H_2O-TEOA (9:1:2)	6	8.9	1.66	84.2
3[b]	Ni@Py-DPEN	CH_3CN-TEOA (4:1)	6	8.19	1.17	87.5

[a] Irradiated with blue LED at λ_{ex} = 470 nm (light power = 70 W/m^2) in CH_3CN-H_2O-TEOA (4:1:2 v/v, 4.0 mL) (entries 1 and 2, Table S1), [b] CH_3CN-TEOA (4:1 v/v, 4.0 mL) (entry 3, Table S1) at 298 K. H_2, HCOOH were not detected.

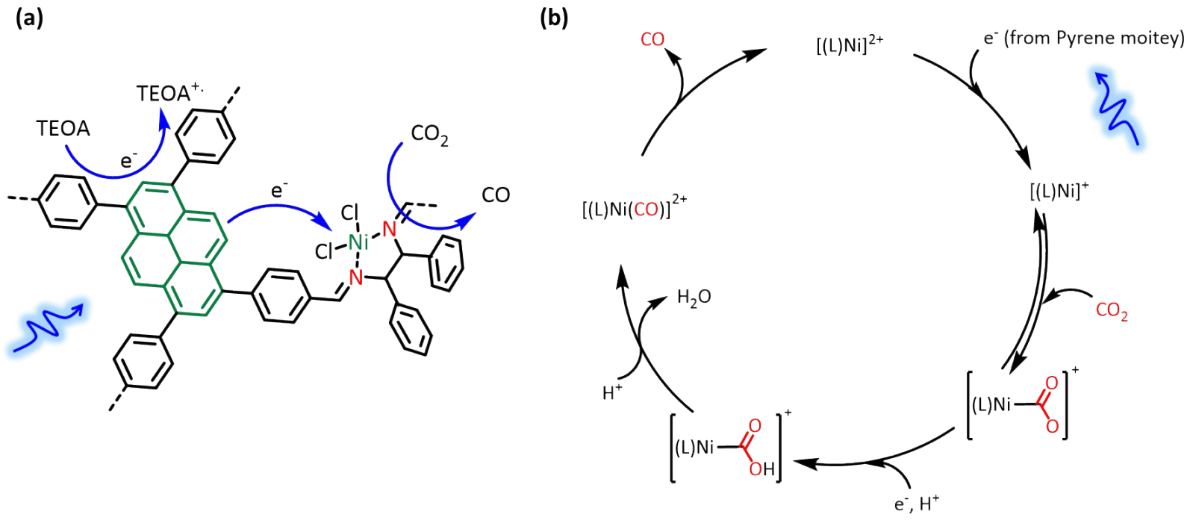

Figure S16. Proposed reaction mechanism; (a) overall mechanism; (b) binding to CO_2 to Ni centre for selective production of CO. [3]

Determination of Apparent quantum yield

The quantum yields (Φ) for the photochemical CO_2 reduction reactions were determined using the following equation: [4]

$$QY(\%) = \frac{\text{product molecules}}{\text{incident photons}} \times 100\%$$

The amount of CO produced was quantified using a calibrated gas chromatograph (GC). The incident photon flux was determined using potassium ferrioxalate $K_3Fe(C_2O_4)_3$ as a chemical actinometer.[5,6] An aqueous solution (4ml, V_1) containing $K_3Fe(C_2O_4)_3$ (0.15 M) and H_2SO_4 (0.05 M) was irradiated using a high-power 470 nm LED light source (Model L-470-HP, MARUTEK: light intensity = 70 W/m^2) under identical conditions to those used for the photocatalytic CO_2 reduction reactions. The irradiation time was kept sufficiently short to ensure that less than 10% of the actinometer decomposed. Prior to each experiment, the output power of the LED light source was measured using a power meter.

After irradiation, an aliquot of 0.180 mL (V_2) was withdrawn and mixed with 2 mL of a buffered phenanthroline solution (0.015 M phenanthroline in 0.5 M H_2SO_4), followed by dilution with distilled water to a final volume of 25 mL (V_3). The absorbance of the resulting solution was recorded at 510 nm, and the number of Fe^{2+} ions generated during irradiation (nFe^{2+}) was calculated using the following equation:

$$nFe^{2+} = \frac{V_1 \times V_3 \times (A-A_0)}{1000 \times V_2 \times e}$$

where V_1 = Volume of actinometer solution irradiated (mL)

V_2 = Volume of aliquot taken for analysis (mL)

V_1 = Final volume to which V_2 is diluted (mL)

A = Measured optical density at 510 nm

A_0 = Measured optical density at 510 nm of non-irradiated sample

e = Experimental value of molar extinction coefficient of Fe^{2+} complex (11100 L mol^{-1} cm^{-1})

Finally, the number of incident photons per second was calculated using the following equation:

$$\text{Number of photons } (s^{-1}) = \frac{6.023 \times 10^{23} \times nFe^{2+}}{\Phi_{\lambda} \times t}$$

Φ_{λ} = Quantum yield of Fe^{2+} formation at 470 nm

t = time of irradiation (s)

Calibration curve

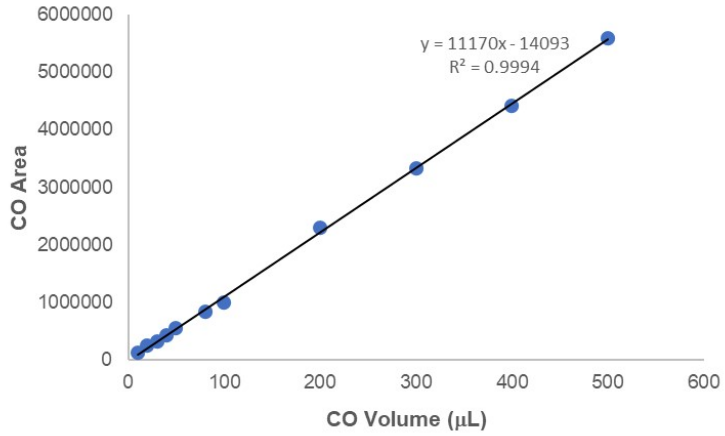

Figure S17. Calibration curve for CO

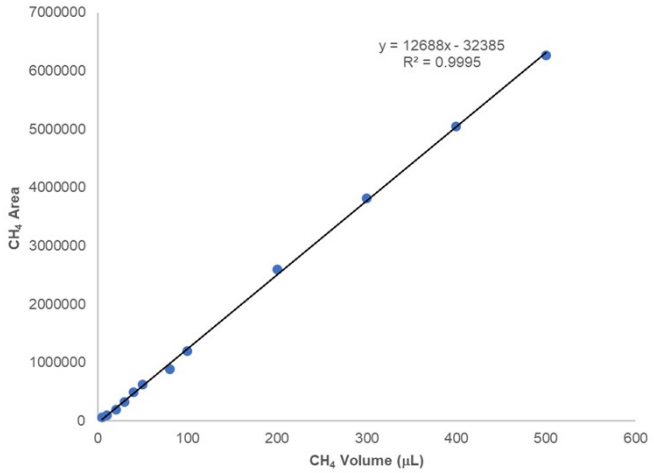

Figure S18. Calibration curve for CH_4.

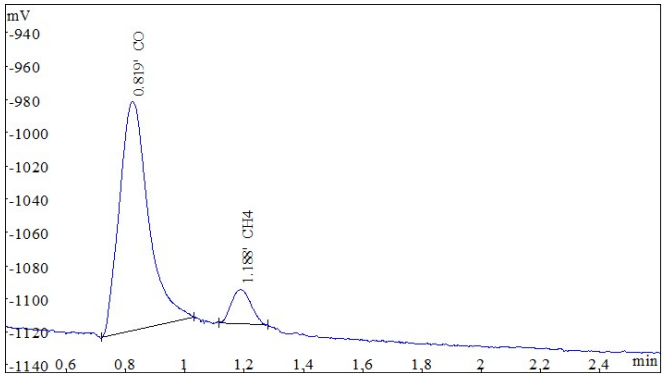

Figure S19. GC trace of reaction mixture after 6 hrs irradiation using (Ni@Py-DPEN) in CH_3CN-H_2O-TEOA (9:1:2, v/v) under CO_2.

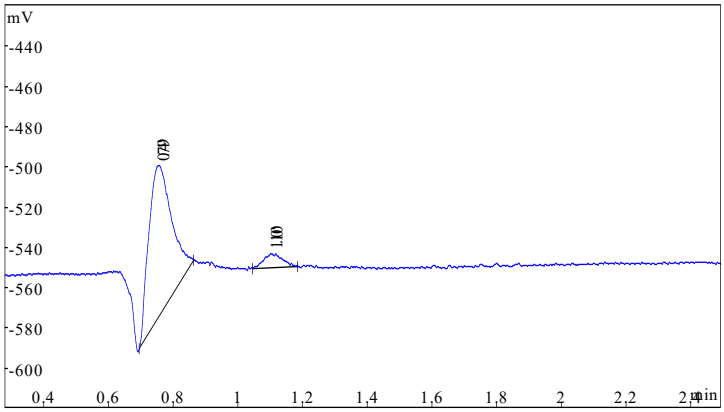

Figure S20. GC trace of reaction mixture after 6 hrs irradiation using Py-DPEN as catalyst in CH_3CN-H_2O-TEOA (9:1:2, v/v) under CO_2.

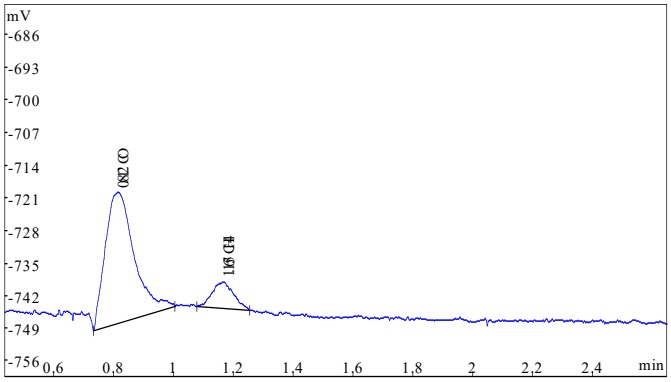

Figure S21. GC trace of reaction mixture after 6 hrs irradiation using Ni@Py-DPEN as catalyst in CH_3CN:TEOA (4:1) under CO_2.

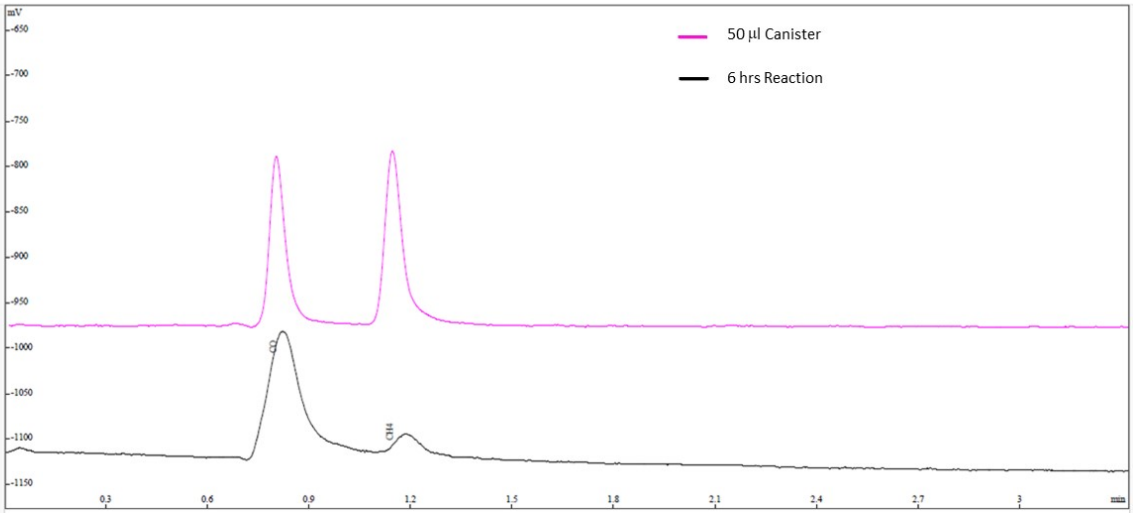

Figure S22. Standard canister 50 µl and reaction mixture after 6 hrs irradiation using Ni@Py-DPEN in CH_3CN-H_2O-TEOA (9:1:2, v/v) under CO_2.

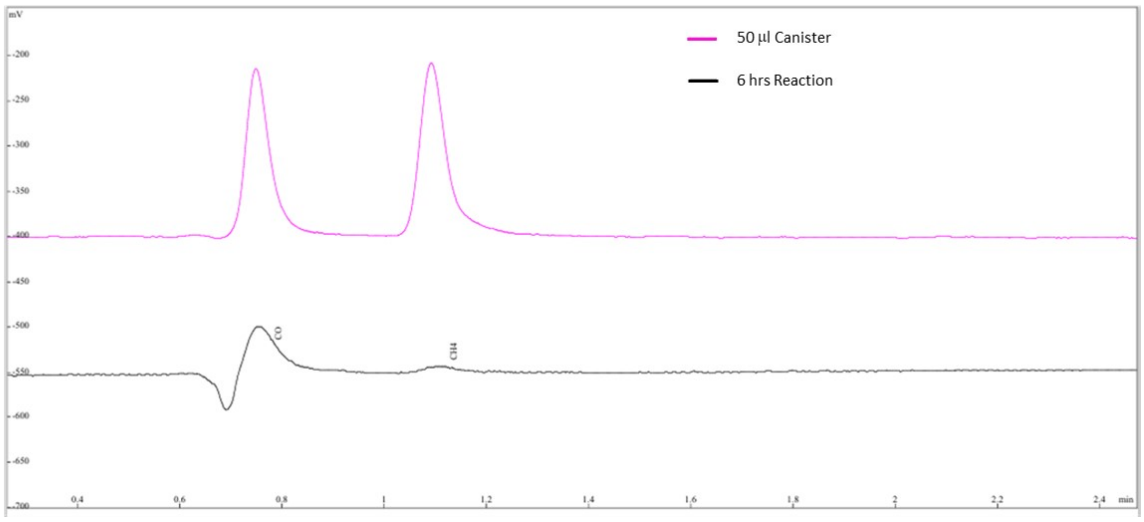

Figure S23. Standard canister 50 µl and reaction mixture after 6 hrs irradiation using Py-DPEN in CH_3CN-H_2O-TEOA (9:1:2, v/v) under CO_2.

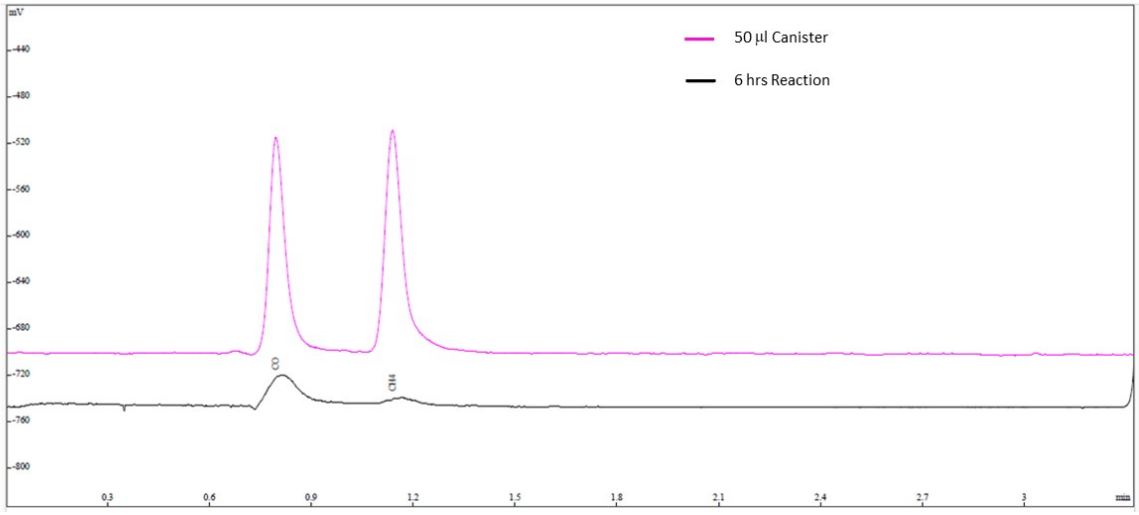

Figure S24. Standard canister 50 µl and reaction mixture after 6 hrs irradiation using Ni@Py-DPEN in CH_3CN-TEOA (4:1, v/v) under CO_2.

References:

1. (a) M. G. Rabbani, A. K. Sekizkardes, O. M. El-Kadri, B. R. Kaafaranic and Hani M. El-Kaderi, *J. Mater. Chem*., 2012, **22**, 25409; (b) Z. Fu, X. Wang, A. M. Gardner, X. Wang, S. Y. Chong, G. Neri, A. J. Cowan, L. Liu, X. Li, A. Vogel, R. Clowes, M. Bilton, L. Chen, R. S. Sprick and A. I. Cooper, *Chem. Sci*., 2020, **11**, 543.
2. (a) H. -S. Xu, S. -Y. Ding, W. -K. An, H. Wu, W. Wang, *J. Am. Chem. Soc*. 2016, **138**, 11489–11492 (b) C. Arqueros, L. Welte, C. Montoro and F. Zamora, *J. Mater. Chem. A*, 2024, **12**, 20121; (c) X. Kong, Z. Wu, M. Strømme, C. Xu, *J. Am. Chem. Soc.* 2024, **146**, 742–751; (d) J. He, X. Jiang, F. Xu, C. Li, Z. Long, H. Chen and X. Hou, Angew Chem. 2021, **60**, 9984-9989.

3. (a) M. Beley, J. P. Collin, R. Ruppert and J. P. Sauvage, *J. Am. Chem. Soc*., 1986, **108**, 7461–7467; (b) J. Song, E. L. Klein, F. Neese and S. Ye, *Inorg. Chem.*, 2014, **53**, 7500–7507; (c) J. A. Hueffel, M. Rigoulet, S. Wellig, T. Sperger, J. S. Ward, K. Rissanen and F. Schoenebeck, *J. Am. Chem. Soc.* 2025, **147**, 30, 26149–26157.
4. D. Ghosh, H. Takeda, D. C. Fabry, Y. Tamaki and O. Ishitani, *ACS Sustainable Chem. Eng*. 2019, **7**, 2648–2657.
5. P. G. Alsabeh, A. Rosas-Hernández, E. Barsch, H. Junge, R. Ludwig and M. Beller, *Catal. Sci. Technol*., 2016, **6**, 3623–3630.
6. A. Rosas-Hernández, P. G. Alsabeh, E. Barsch, H. Junge, R. Ludwig and M. Beller, *Chem. Commun*., 2016, **52**, 8393–8396.